JMEPEG (2023) 32:1966–1973
https://doi.org/10.1007/s11665-022-07222-4

1059-9495/$19.00

TECHNICAL ARTICLE

Fabricating Efficient and Biocompatible Filament for Material Extrusion-Based Low-Cost Additive Manufacturing: A Case Study with Steel

Tridib K. Sinha, Harshada R. Chothe, Jin Hwan Lim, Jung Gi Kim, Taekyung Lee, Taehyun Nam, and Jeong Seok Oh

Submitted: 9 February 2022 / Revised: 10 May 2022 / Accepted: 17 June 2022 / Published online: 17 August 2022

The production of various 3D-printed metal or ceramic parts via fused deposition modeling (FDM) or fused filament fabrication (FFF) is gaining tremendous interest. This is because FDM or FFF are cost-effective and have comparatively faster processability. FDM or FFF are material extrusion-based additive manufacturing processes in which the filament is extruded through a nozzle at a high temperature, and the object is formed by its layer-by-layer deposition. Irrespective of the metal/ceramic precursors, the choice of binder/carrier is crucial for developing 3D-printed parts using FDM of FFF techniques. The optimization of processing parameters determines the perfectness of the binder/carrier chosen for successful 3D printing. In the case of multi-component metal alloy preparation, the binder tightly holds the alloying components close to each other and helps to maintain their stoichiometry. A suitable carrier holds ample alloying components while retaining enough flexibility and strength to the filament for printing. Compatibility between the binder and carrier can synergistically improve the 3D printing. Polyvinyl pyrrolidone (PVP) has been chosen as a highly processable and biocompatible binder in this work, while thermoplastic polyurethane (TPU) is a biocompatible carrier for the PVP-bound metal. The metal powder having a composition of Fe-1.5Ni-1.5Cu (as per the wt.%) has been used to investigate the efficacy of the binder and carrier. The binding of metal powder with PVP dispersion, melt mixing of PVP-bound metal powder with the TPU, extrusion of the TPU/PVP-bound metal (TPM) composite, 3D printing of the extruded filament (containing 40 vol.%, i.e., 82 wt.% of metal) using a low-cost 3D printer, and debinding of the printed product/s at different heating conditions have been thoroughly optimized and successfully standardized.

Keywords binder, carrier, fused deposition modeling (FDM), metal 3D printing, PVP, TPU

1. Introduction

Nowadays, extrusion of materials (e.g., ceramics, metals, etc.) using polymers as binder/carrier is being attempted enormously for developing various low-cost customized products of desired shapes and sizes via formation of layer-by-layer assembly of the components as per the computer-aided-design (CAD) data using the additive manufacturing (AM) or three-dimensional (3D) printing technique (Ref 1-3). In particular, the 3D printing technique comprises with extrusion of polymers, or their composites followed by their layer-by-layer deposition, is known as fused deposition modeling (FDM) or fused filament fabrication (FFF) technique (Ref 4-6). Various research has been reported recently on the development of objects using composite filaments loaded with different metals/ceramics (e.g., steel, titanium, silica, silicon nitride, alumina, zirconia, lead zirconate titanate, etc.) via the FDM/FFF technique (Ref 1, 2, 4-11). There is no such restriction on selecting the metal/ceramics that would be bonded during post-printed sintering; however, the binder/carrier plays a major role in developing the pre-sintered 3D-printed object. Generally, a thermoplastic compound comprising polymeric materials filled with a high volume of metal/ceramic as a feedstock is formulated and extruded to a printable filament (Ref 4, 12). The filaments of various diameter ranges are then used for 3D printing. During 3D printing, the polymer (binder/carrier) enables the shaping of the 3D-printed parts (Ref 13). Homogenous distribution of the non-polymeric materials (e.g., metal) within the polymer matrix is typically needed to ensure the repeatability and reproducibility of the 3D-printed parts. Good metal-to-binder/carrier interaction is thus needed to realize homogeneity in the composites containing non-polymeric materials within the polymer matrix (Ref 14, 15). Another important feature of polymer is its comparatively enhanced load-bearing capacity, which can be accomplished by introducing some rubbery properties to the polymer. Otherwise, at high metal/ceramic loading, the extruded filament is expected to be brittle, which will remain complicated for further processing. Again, the biocompatible polymer is highly desired for the 3D printing of

Tridib K. Sinha and Harshada R. Chothe have equally contributed this research work.

Tridib K. Sinha, Department of Materials Engineering and Convergence Technology, RIGET, Gyeongsang National University, 501 Jinju-daero, Jinju 52828, South Korea; and Department of Applied Sciences, School of Engineering, University of Petroleum and Energy Studies (UPES), Energy Acres Building, Dehradun, Uttarakhand, India; **Harshada R. Chothe, Jin Hwan Lim, Jung Gi Kim, Taehyun Nam,** and **Jeong Seok Oh**, Department of Materials Engineering and Convergence Technology, RIGET, Gyeongsang National University, 501 Jinju-daero, Jinju 52828, South Korea; **Taekyung Lee**, School of Mechanical Engineering, Pusan National University, Busan 46241, South Korea. Contact e-mails: tahynam@gnu.ac.kr and ohjs@gnu.ac.kr.

biomedical products. In this regard, biocompatible thermoplastic elastomers (TPE) with abundant functional groups may be considered suitable candidature to be applied as binder/carrier. For processing of metal-alloy containing multiple metals, the component metals must be tightly held closer to each other, and their stoichiometry is desired to be well maintained. Although many attempts are being made to accomplish the metal/ceramic 3D printing using the polymer-based binder/carrier, their chemical composition is yet to be known by the researchers/industrialists because the binder composition is still an intellectual property of the suppliers' organizations (Ref 16, 17). This fact limits the progressive up-gradation in research and development (R&D). On the other hand, the basic requirement of 3D printing of the filament loaded with metal/ceramic is its continuous flowability to develop the desired structure having a homogenous composition, for which the 3D printer companies are sticking with the development of low-cost 3D printers enabling the proper printing of metal/ceramic-loaded polymeric filament. For printing the filaments of polymers only, the process is very simple, which works via melting of polymers, flowing the melt through the nozzle, and finally designing the printed parts. The process is commonly known as fused deposition modeling (FDM) (Ref 18, 19). In the case of metal/ceramic-loaded polymer printing, it is highly desired that the non-polymeric parts will not be phased-out of the melted polymer binder/carrier and flow along with the polymer. If the metals/ceramics are phase-out, they will clog the nozzle, and the process will not be continuous.

In this study, a 3D printable filament has been developed by using a bio-compatible thermoplastic elastomer, i.e., TPU, as a carrier while another biocompatible and highly processable amorphous polymer, i.e., PVP as a binder for the alloying elements of steel-alloy (i.e., Fe-1.5Ni-1.5Cu (as per the wt.%)). The processing conditions for developing the printable filament via melt mixing of PVP-bound metal with the TPU followed by extrusion of the TPU/PVP-bound metal (TPM) composite have been thoroughly investigated and optimized. A low-cost FDM 3D printer has been used to investigate the printability of the TPM composite filament under various printing conditions (e.g., nozzle diameter, printing temperature, filament diameter, etc.). Also, this study shows the debinding of 40 vol% filled filament at different heating rates.

2. Experimental

2.1 Materials

The metal powders used in this work are high quality (more than 99% purity) Iron (Fe-75 μm), Copper (Cu-10 μm), and Nickel (Ni-5-15 μm), which were obtained from Thermo Fisher Scientific. The polymers, i.e., polyvinyl pyrrolidone (PVP-K30, Sokolan) and thermoplastic polyurethane (TPU) (Elastollan 1190A), were procured from the BASF.

2.2 Mixing of Alloying Metal Powders

Metals with a composition of Fe-1.5Cu-1.5Ni (by wt.%) are used to investigate the processing steps toward developing metal alloy-based 3D-printed objects. The mixing of iron, copper, and nickel has been done by ball milling without balls for 5 h at 350 rpm.

2.3 Preparation of Binder Solution and PVP-Bound Metal Powder

PVP is used as a biocompatible binder to bind the mixed metal powder. 0.5 wt.% of PVP (according to the weight of the metal powder mixture) was dissolved in ethanol through continuous stirring using a magnetic stirrer. Later the mixed metal powder was added to the clear solution of PVP and mixed using a mechanical stirrer until the solution became a thick paste due to evaporation of the solvent (i.e., ethanol), and further dried in an oven at 50 °C (till the complete removal of solvent). During drying, every 20 min, the PVP-bound metal powder mixture was hand-mixed for 2 min to avoid accumulation and ensure the homogenous size of the PVP-bound metal powder. The coated metal powder was ground using mortar-pestle and sieved through 30 mesh (i.e., 600 μm) sieves to separate the bigger particles.

2.4 Melt Mixing of TPU (Carrier) and PVP-Bound Metal Powder

TPU/PVP-bound metal (i.e., TPM) composites were prepared via melt mixing of PVP-bound metal powder with the carrier (i.e., TPU) in an internal mixer fitted with counter-rotating roller rotors a mixing chamber volume of 160 cm^3. Various samples of different metal-to-polymer ratio (e.g., 10:20, 20:80, 30:70, 40:60 (as per the volume ratio) equivalent to 44:56, 67:36, 75:25, 82:18 (as per the weight ratio) have been prepared in this investigation. TPU/PVP-bound metal (i.e., TPM) composites of lower metal content was also formulated for comparison. Mixing was examined at different temperatures (near the melting temperature of TPU) for different mixing times under variable rotor speed (rpm) to realize the suitable mixing condition to be well-fitted for the next steps. It was observed that the melt mixing parameters plays a crucial role in the filament quality after extrusion. For instance, after melt mixing at a higher temperature, higher rotor speed, and longer period, the carrier was found to degrade, resulting in its reduced ability to extrude and carrying capacity of the metal powder. Therefore, this study's preferred operating conditions for melt mixing are standardized at 160 °C, 25 rpm, and 20 min (max.), respectively.

2.5 Grinding and Sieving of TPU-Metal Composite

The melt mixed TPM composite was further ground into smaller size using a grinder to make it extrudable toward developing a filament of expected metal-to-polymer ratio. The fine particles were separated out using 30 mesh sieves to ensure the formation of a better filament.

2.6 Fabrication of 3D Printable Metal-Filament

The ground TPU-metal composite of nearly homogenous size was used to prepare the filament for 3D printing. The filaments having a diameter in the range of 1.65 $\pm$ 0.5 and 1.75 $\pm$ 0.5 mm was prepared using (Fila Bot EX2 single screw extruder) equipped with a round die at 190 °C under 5 and 8 rpm screw speed. The extruded filament was then passed through an air path for cooling and collected using a spooler. It has been found that the extruder was unable to extrude well the composite obtained at a mixing condition of 190 °C or higher temperature, while that of 160 °C was found to be well extruded. Various temperatures (e.g., 180, 190, and 200 °C) and

screw speeds (e.g., 8, 5, and 3 rpm) were examined to standardize the processing condition of filament fabrication, and the productive condition was optimized as 190 °C processing temperature under 5 and 8 rpm screw speed. At a screw speed higher than 8 rpm, the filaments having a diameter of more than 1.8 mm were obtained. At a screw speed lower than 5 rpm (i.e., 3 rpm), the filament of the desired diameter was unable to collect. The required diameter adjustable for the 3D printer is set as 1.5-1.8 mm. The diameter of extruded filament was measured by a micrometer (i.e., Mitutoyo absolute, Japan).

2.7 3D Printing

Once the suitable processing conditions were selected for both the internal mixer and extruder, the filament obtained at 190 °C under 5 and 8 rpm was subjected to 3D printing using an FDM 3D printer (Rokit, South Korea) equipped with the nozzles of 0.6 mm and 1.0 mm diameter. Several processing temperatures were examined to realize the suitable printing temperature. The fully dense (i.e., 100% infill) 3D-printed objects (i.e., cube) were prepared with a linear infill pattern having a layer height of 1 mm. Printing of one cube took 15 min and 0.587 m of the filament. Figure 1 schematically represents all the steps toward successfully developing a 3D-printed structure from the TPM composite filament.

2.8 Thermal Debinding

The 3D-printed specimens were further treated by thermal debinding under an argon (Ar) atmosphere. The specimens were heated from room temperature to 1000 °C with 0.5, 0.3 and 0.1 °C/min heating rates to ensure neck formation during debinding.

3. Characterizations

The coating of PVP over the metal surfaces through the noncovalent interaction resulting in the formation of PVP-bound metal has been investigated using the FT-IR spectra (Thermo Scientific iD5 spectrophotometer) recorded from 500-3500 cm^{-1} in ATR mode. The PVP-bound metal particle has again been characterized using the x-ray diffraction (XRD, Bruker D2 phaser) analysis to confirm their formation through the noncovalent electrostatic interaction. Thermal characterizations (i.e., TGA) have been pursued to confer the metal to polymer ratio in the TPM composite using the TA instrument at a heating rate of 10 °C/min under N_2 atmosphere. Gravimetric analysis was accomplished to optimize the flowability of the filament to realize a better 3D printing structure. Morphological feature of the PVP-bound metal, TPM composite filament, and 3D-printed object was studied to know about the dispersion of the PVP-bound metal within the TPU matrix and compatibility of the metal with the binder and the bound metal with the TPU matrix, using SEM (Philips XL30S) analysis. Also, the neck formation and binder removal after debinding were confirmed using SEM analysis.

4. Results and Discussion

PVP as binder and TPU as a carrier in this work has been chosen to satisfy the aforementioned prospectives of 3D printable metallic filament. Steel alloy containing Fe, Ni, and Cu (Fe-1.5Cu-1.5Ni as per the weight ratio) is taken as the target alloy to be 3D-printed. Because of its abundant binding

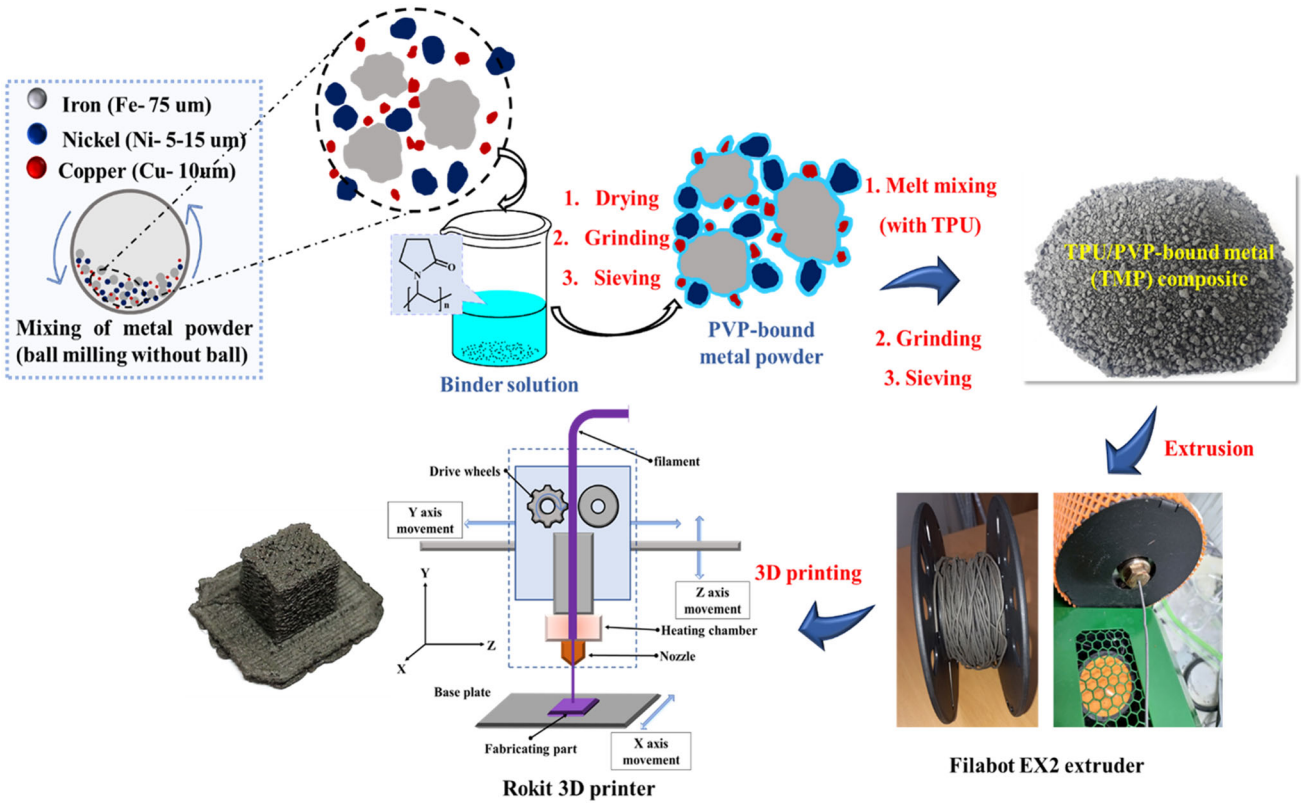

Fig. 1 Schematic representation of the development of a 3D-printed structure from the TPM composite filament

efficacy to the metal through the noncovalent metal-PVP interaction (Ref 20-22), PVP was found to bind the alloying metals well, resulting in the formation of comparatively larger particles which were found to be free-flowing over the surface of tissue paper. In contrast, the non-bound metal powders adhered to the paper surface (as demonstrated in Fig. 2a). As a consequence of binding through noncovalent interaction, the stretching frequencies of the functional groups (mainly the carbonyl group) were found to be shifted, which affirms the PVP-metal interaction and formation of the PVP-bound metal (shown in Fig. 2b). The FT-IR was carried out in the range of 500-3500 cm^{-1}. PVP presents the peaks at 2835-3035, ~ 1650, ~ 1400, ~ 1245, and ~ 1065 cm^{-1}, corresponding to the stretching frequency of C-H (asymmetric stretching) and C = O (carbonyl), bending frequency of CH_2, C-N stretching, and C-O stretching while these peaks are shifted for the PVP-bound metal, e.g., shift of C = O stretching frequency from ~ 1650 to 1660 cm^{-1} employing the existence of metal-binder interaction (Ref 22-24). The broad and intense peak at lower wavenumber (i.e., at around 650 cm^{-1}) may be due to the presence of alloying metals. In the case of XRD analysis, the shift in characteristic 2 theta values of the metal components (i.e., Fe, Cu, and Ni) was observed for the PVP-bound metal particle, which again infers the binding of metal with the PVP through noncovalent interaction (Fig. 2c) (Ref 25, 26). The decrease in peak intensities also replicates PVP coating over metal surfaces. From the morphological characterization (i.e., SEM) and related EDS analysis, the elemental metals are found to bind together, having almost a desired stoichiometry (i.e., metal-to-metal weight ratio). The weight ratio of the metal after the binding was found similar to that of the non-bound metals (i.e., Fe-1.5 Ni-1.5 Cu).

After formulation of the PVP-bound metal particles, these were subjected to mix with the carrier, i.e., TPU via melt mixing using an internal mixer. The functional group of PVP over the metal surface can have abundant interaction (both the polar–polar and nonpolar–nonpolar) with the TPU functionalities, facilitating the well dispersion of the bound-metal particles within the carrier matrix. During melt mixing, it is highly required that the elastic property of TPU will be intact so that the extruded filament made of the melt mixed TPU/PVP-bound metal (i.e., TPM) composite will be flexible enough to handle. In typical cases, melt mixing is recommended at around the operating temperature of the composite components. But, in the case of TPU, the temperature, rotor speed, and mixing time were found to synergistically influence the property of the TPM

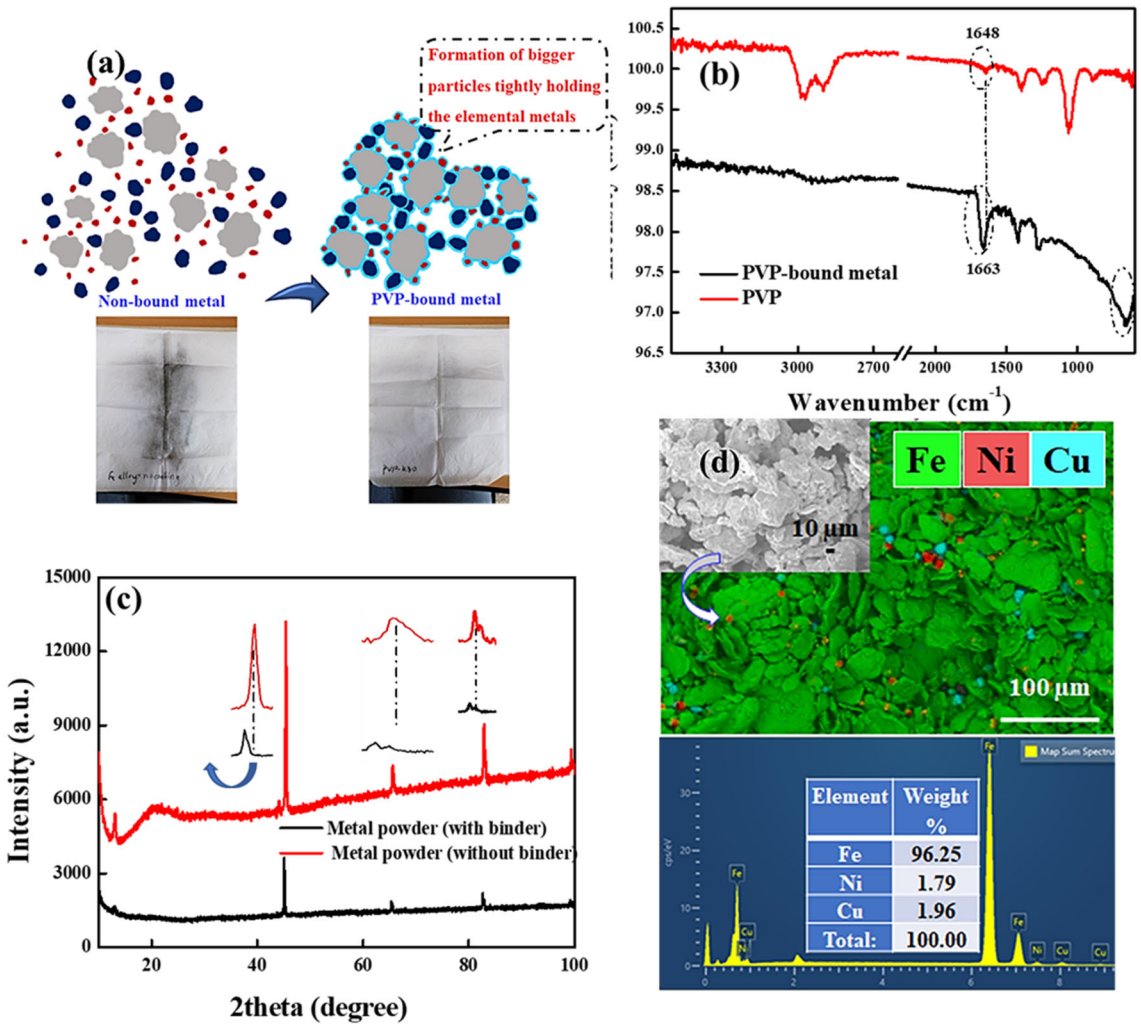

Fig. 2 (a) Comparative flowability of metal (with and without binder), (b) FT-IR spectra of PVP and PVP-bound metal, (c) XRD of metal powder with and without binder (d) SEM image and EDS analysis of the PVP-bound metal

composite. The mixing condition was optimized by checking the quality of the extruded filament. During extrusion of the melt mixed composite, it is highly desirable that the extruded filament should have good mechanical and rheological properties. The trajectory of the extruded filament can be considered as a benchmark to realize its quality. For instance, the excellent quality filament was enabled from the composite obtained at 160 °C mixing temperature for 20 min mixing under 25 rpm rotor speed. An increase in either temperature, rotor speed, or mixing time was found to produce bad quality filament. The filament obtained under these increased conditions, the extrusion results in either brittle filament or no filament to be collected properly. Notably, the rubbery property of the composite has been found to deteriorate under these increased conditions. It can be said that the polymeric entanglements may tear due to aging under these improved conditions. For clarity, Fig. 3(a) shows the filament quality of the melt mixed TPM composites obtained at different temperatures. The extruding parameter was fixed at 190 °C processing temperature under 5 and 8 rpm screw speed during extrusion. Alteration in temperature, the filament quality was found to deteriorate. At lower temperatures, the filament surface was rough, whereas, at higher temperatures, the filament was brittle. Figure 3(b) (shows) the filament quality obtained at different extrusion temperatures and 5 rpm screw speed. The metal-to-polymer ratio was investigated by TGA analysis and found to be well-matched with the designed formula.

Figure 3(c) represents the TGA curves of different filaments (obtained at 190 °C and 5 rpm) having different metal-to-polymer ratios, from which it can be noticed that the wt.% of metal content in the filaments is nearly similar to that of the calculated values. This observation supports the potential of TPU and PVP as carriers and binders, respectively. Figure 3(d) shows the SEM images of the extruded filament (obtained at 190 °C), from which it can be noticed that the metals are impregnated with the honeycomb structure of the polymer matrix. From the EDS analysis, the metal-to-metal ratio was found nearly similar to that of the calculated value in this structure. The slight deviation may be correlated with the densities of the metal components and their orientation laid by their electron affinity and variation in metal-polymer noncovalent interaction. Following the conditions optimized in this investigation, we prepared good quality filaments with a diameter ranging from 1.65 ± 0.5 to 1.75 ± 0.5 mm at 190 °C processing temperature under 5 and 8 rpm screw speeds were found to efficiently produce the 3D-printed objects through the nozzle of 1.0 mm diameter. In the case of a 0.6 mm nozzle, clogging was observed.

The printing temperature being a vital factor in developing the desired high-resolution object, has been optimized during the 3D printing (Ref 27, 28). In this case, the filament is composed of two different polymers, one is TPE (i.e., TPU), and another is amorphous (i.e., PVP), interacting with each other through noncovalent interaction. With increasing the

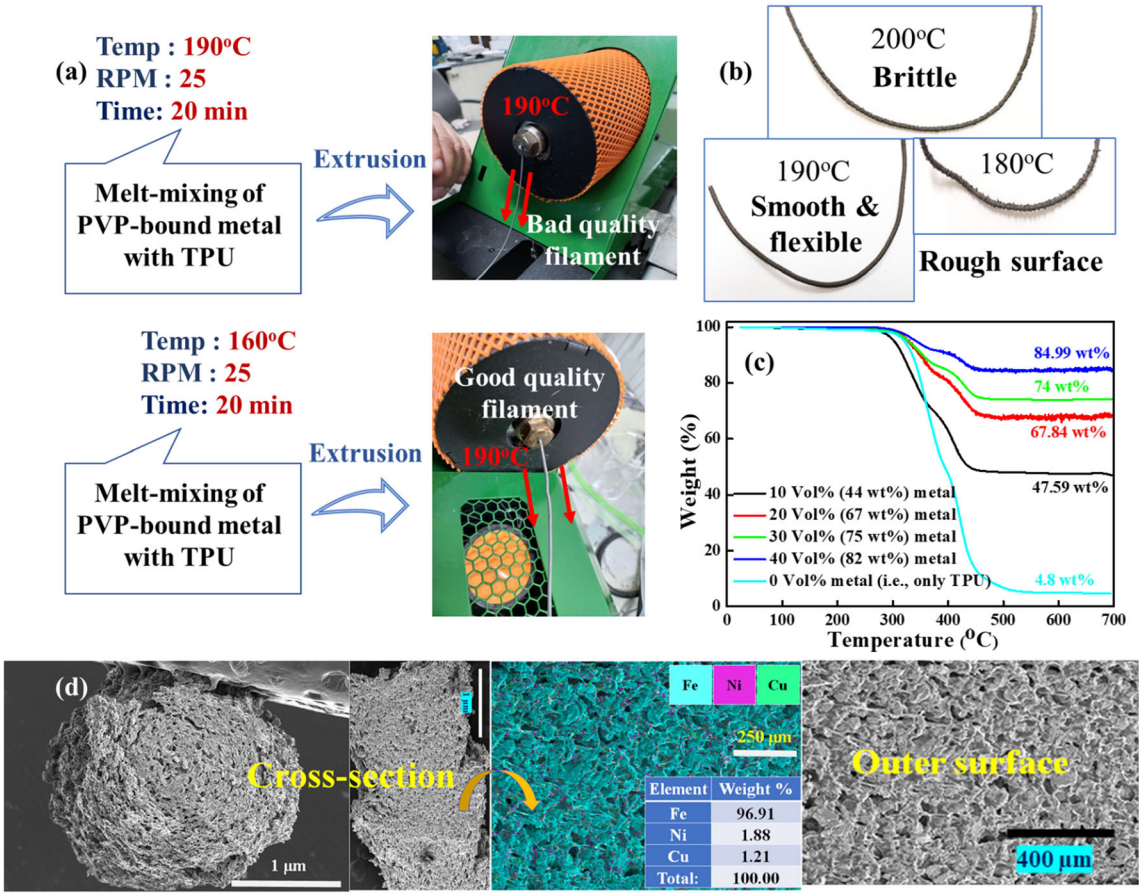

Fig. 3 (a) Filament quality of the TPM composite obtained at various melt mixing conditions, (b) Filament quality obtained at different extrusion temperatures, (c) TGA of filaments containing different metal-to-polymer ratios, (d) SEM images, and EDS analysis of the TPM filament obtained at 190 °C processing temperature and 5 rpm screw speed

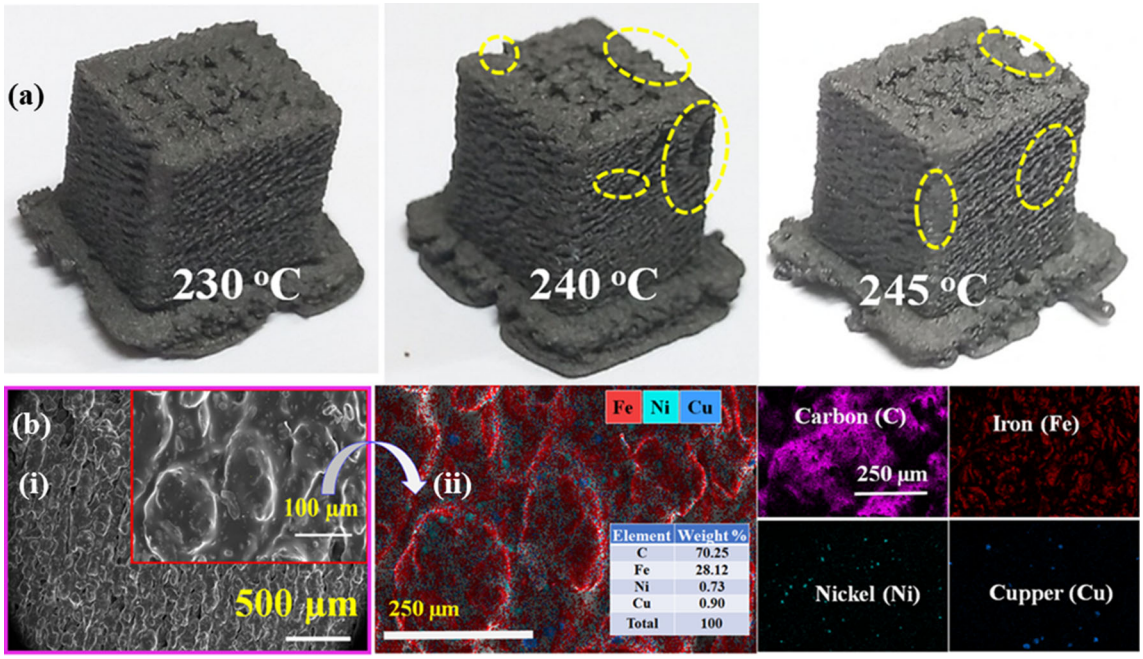

Fig. 4 (a)TPM-based 3D-printed objects under various printing conditions and (b) SEM and EDS analysis of 3D-printed object at 230 °C temperature

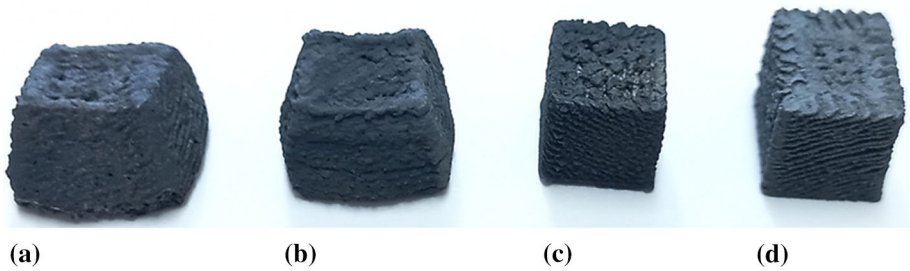

Fig. 5 Debound objects with different heating rates (a) 0.5 °C/min, (b) 0.3 °C/min and (c) 0.1 °C/min, and (d) object before debinding

temperature, the melt flowability of TPE is supposed to be increased. Consequently, the interaction between the flowable TPE (TPU) and non-flowable amorphous PVP may decrease, resulting in aggregation of the PVP-bound metal and clogging of the nozzle. Also, the resolution of the printed object may be hampered. In this work, various printing temperatures (e.g., 230, 240, and 245 °C) have been examined, and the 230 °C printing temperature was standardized for successful and repeatable 3D printing. In the case of higher operating temperatures, the 3D printing was not repeatable due to clogging. Also, the objects obtained at higher temperatures showed defective formation compared with 230 °C. Figure 4(a) shows the quality of the printed objects (i.e., cube) obtained at various printing temperatures using the 1.0 mm nozzle. The defective portions of the 3D-printed cubes obtained at higher temperatures are highlighted with yellow dotted circles. The SEM images of the cube's surface printed at 230 °C are shown in Fig. 4(b). Coating of melted polymer over the surface of PVP-bound metal can be observed from the inset of Fig. 4(b) (i), which supports the presence of interaction between the TPU and PVP during 3D printing. From the color images (as shown in Fig. 4b (ii), the coating of polymers as a sheet covering the metals is visible. Consequently, the wt.% of total metal on the surface of the printed object is found to be reduced than that of the calculated value.

During thermal debinding, the polymer will melts and evaporates at a higher temperature. However, the higher heating rate ($>$ 1 °C/min) can lead to disturbed structure of the printed components (Ref 16). In this work, we preferred low heating rates for debinding of the 3D-printed objects at 1000 °C debinding temperature. The thermal debining was performed to remove the binder with three different heating rates, 0.5, 0.3 and 0.1 °C/min, respectively, as shown in Fig. 5. After the thermal debinding at 0.5 and 0.3 °C/min the specimen shape was changed, but in the case of 0.1 °C/min, the specimen maintained the same shape without bloating or cracking. The specimen shrunk around 12% of its volume compared to the 3D-printed sample. Also, the weight loss was $\sim$ 18%, equivalent to the amount of binder present in 3D-printed objects.

Debinding helps the object to retain its structure (through neck formation) even after removing the binder Fig. 6(a) and (b) shows the 3D-printed specimen before and after debinding at 1000 °C. After the thermal debinding, the binder was successfully removed, and neck formation was started. Further, the EDS analysis also confirmed the composition of iron alloys was almost equal to the original ratio, as shown in Fig. 6(c).

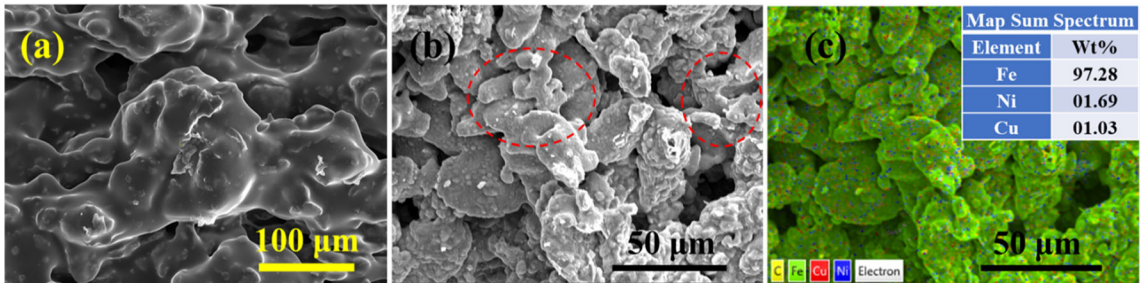

Fig. 6 SEM images of (a) 3D-printed object before debinding and (b) after debinding, (c) EDS analysis of debound object

Many literatures confirmed the debinding of 3D-printed object with high metal content (> 40vol%) (Ref 16, 17, 29, 30) but from this study it is confirmed that even 40 vol% metal-filled filament can show good debinding.

5. Conclusions

In this investigation, materials composition, processing steps, and conditions have been optimized and standardized for successful 3D printing of metal-loaded polymer composite. PVP as a biocompatible binder and TPU as a biocompatible carrier has been found to prepare the 3D printable filaments for developing various 3D-printed metal structures of intricate designs, especially for biomedical purposes. It is noteworthy that a low-cost traditional FDM printer has successfully printed the TPM composite filaments, provided some modifications on filament property (especially diameter), nozzle diameter, printing temperatures, etc., have been done. From this study the debinding of 40 vol% metal-filled filament is performed sucessfully.

Acknowledgments

This work was supported by the National Research Foundation of Korea (NRF) grant funded by the Korean government (MSIT) (2020R1A4A3079417).

Conflict of interest

The authors declare no financial/commercial conflicts of interest.

References

1. Z. Chen, Z. Li, J. Li, C. Liu, C. Lao, Y. Fu, C. Liu, Y. Li, P. Wang, and Y. He, 3D Printing of Ceramics: A Review, *J. Eur. Ceram. Soc.*, 2019, **39**(4), p 661–687
2. C. Buchanan and L. Gardner, Metal 3D Printing in Construction: A Review of Methods, Research, Applications, Opportunities and Challenges, *Eng. Struct.*, 2019, **180**, p 332–348
3. A. Bandyopadhyay, K.D. Traxel, M. Lang, M. Juhasz, N. Eliaz, and S. Bose, Alloy Design Via Additive Manufacturing: Advantages, Challenges, Applications and Perspectives, *Mater. Today*, 2022, **52**, p 207–224
4. S. Cano, J. Gonzalez-Gutierrez, J. Sapkota, M. Spoerk, F. Arbeiter, S. Schuschnigg, C. Holzer, and C. Kukla, Additive Manufacturing of Zirconia Parts by Fused Filament Fabrication and Solvent Debinding: Selection of Binder Formulation, *Addit. Manuf.*, 2019, **26**, p 117–128
5. J. Abel, U. Scheithauer, T. Janics, S. Hampel, S. Cano, A. Müller-Köhn, A. Günther, C. Kukla, and T. Moritz, Fused Filament Fabrication (FFF) of Metal-Ceramic Components, *J. Vis. Exp*, 2019, **143**, p e57693
6. C. Tosto, J. Tirillò, F. Sarasini and G. Cicala, Hybrid Metal/Polymer Filaments for Fused Filament Fabrication (FFF) to Print Metal Parts, *Appl. Sci.*, 2021, **11**(4), p 1444
7. M.K. Agarwala, V.R. Jamalabad, N.A. Langrana, A. Safari, P.J. Whalen, S.C. Danforth, (1996) Structural Quality of Parts Processed by Fused Deposition, *Rapid prototyping journal*
8. D. Nötzel, R. Eickhoff, and T. Hanemann, Fused Filament Fabrication of Small Ceramic Components, *Materials*, 2018, **11**(8), p 1463
9. M. Jafari, W. Han, F. Mohammadi, A. Safari, S. Danforth, N. Langrana, (2000) A Novel System for Fused Deposition of Advanced Multiple Ceramics, *Rapid Prototyping Journal*
10. P. Singh, V.K. Balla, A. Tofangchi, S.V. Atre, and K.H. Kate, Printability Studies of Ti-6Al-4V by Metal Fused Filament Fabrication (MF3), *Int. J. Refract Metal Hard Mater.*, 2020, **91**, p 105249
11. R. Singh, H. Singh, I. Farina, F. Colangelo, and F. Fraternali, On the Additive Manufacturing of an Energy Storage Device from Recycled Material, *Compos. B Eng.*, 2019, **156**, p 259–265
12. J. Gonzalez-Gutierrez, S. Cano, S. Schuschnigg, C. Kukla, J. Sapkota, and C. Holzer, Additive Manufacturing of Metallic and Ceramic Components by the Material Extrusion of Highly-Filled Polymers: A Review and Future Perspectives, *Materials*, 2018, **11**(5), p 840
13. F. Wang, E.B. Tankus, F. Santarella, N. Rohr, N. Sharma, S. Märtin, M. Michalscheck, M. Maintz, S. Cao, and F.M. Thieringer, Fabrication and Characterization of PCL/HA Filament as a 3D Printing Material Using Thermal Extrusion Technology for Bone Tissue Engineering, *Polymers*, 2022, **14**(4), p 669
14. D.E. Bergbreiter, J.D. Frels, C. Li, Soluble polymeric ligands for metal complexation and catalyst recovery, Macromolecular Symposia, 2003, Wiley Online Library, pp 113–140
15. A.C. Bailey, 2018 "In-Situ Densification of Metal Binder Jet Printed Components via Nanoparticles," North Carolina Agricultural and Technical State University
16. Y. Thompson, J. Gonzalez-Gutierrez, C. Kukla, and P. Felfer, Fused Filament Fabrication, Debinding and Sintering as a Low Cost Additive Manufacturing Method of 316L Stainless Steel, *Addit. Manuf.*, 2019, **30**, p 100861
17. J. Gonzalez-Gutierrez, D. Godec, C. Kukla, T. Schlauf, C. Burkhardt, C. Holzer, 2017 Shaping, Debinding and Sintering of Steel Components via Fused Filament Fabrication, Proceedings of the 16th International Scientific Conference on Production Engineering, pp 99–104
18. S. Wickramasinghe, T. Do, and P. Tran, FDM-based 3D Printing of Polymer and Associated Composite: A Review on Mechanical Properties, Defects and Treatments, *Polymers*, 2020, **12**(7), p 1529
19. T.J. Word, A. Guerrero and D. Roberson, Novel Polymer Materials Systems to Expand the Capabilities of FDM™-Type Additive Manufacturing, *MRS Commun.*, 2021, **11**(2), p 1–17
20. X. Li, H. Deng, Z. Li, H. Xiu, X. Qi, Q. Zhang, K. Wang, F. Chen, and Q. Fu, Graphene/Thermoplastic Polyurethane Nanocomposites: Surface Modification of Graphene through Oxidation, Polyvinyl Pyrrolidone Coating and Reduction, *Compos. A Appl. Sci. Manuf.*, 2015, **68**, p 264–275
21. H.-Y. Mi, Z. Li, L.-S. Turng, Y. Sun, and S. Gong, Silver Nanowire/Thermoplastic Polyurethane Elastomer Nanocomposites: Thermal,

Mechanical, and Dielectric Properties, *Mater. Des.*, 2014, **1980–2015**(56), p 398–404
22. M. Shahmiri, N.A. Ibrahim, W.M.Z.W. Yunus, K. Shameli, N. Zainuddin, and H. Jahangirian, Synthesis and Characterization of CuO Nanosheets in Polyvinylpyrrolidone by Quick Precipitation Method, *Adv. Sci. Eng. Med.*, 2013, **5**(3), p 193–197
23. T.K. Sinha, J.H. Lim, H.R. Chothe, J.G. Kim, T. Nam, T. Lee, and J.S. Oh, Polyvinyl Pyrrolidone (PVP) as an Efficient and Biocompatible Binder for Metal Alloy Processing: A Case Study with Ti-20Zr-11Nb-3Sn, *J. Appl. Polym. Sci.*, 2022, **139**(25), p e52396
24. M. Kozakiewicz-Latała, K.P. Nartowski, A. Dominik, K. Malec, A.M. Gołkowska, A. Złocińska, M. Rusińska, P. Szymczyk-Ziółkowska, G. Ziółkowski, A. Górniak, and B. Karolewicz, Binder Jetting 3D Printing of Challenging Medicines: From Low Dose Tablets to Hydrophobic Molecules, *Eur. J. Pharm. Biopharm.*, 2022, **170**, p 144–159
25. M. Aslan, D. Weingarth, N. Jäckel, J. Atchison, I. Grobelsek, and V. Presser, Polyvinylpyrrolidone as Binder for Castable Supercapacitor Electrodes with High Electrochemical Performance in Organic Electrolytes, *J. Power Sources*, 2014, **266**, p 374–383
26. J. Zhang and D.J. Young, Contributions of Carbon Permeation and Graphite Nucleation to the Austenite Dusting Reaction: A Study of Model Fe–Ni–Cu Alloys, *Corros. Sci.*, 2012, **56**, p 184–193
27. G. Singh, J.-M. Missiaen, D. Bouvard, and J.-M. Chaix, Copper Extrusion 3D Printing Using Metal Injection Moulding Feedstock: Analysis of Process Parameters for Green Density and Surface Roughness Optimization, *Addit. Manuf.*, 2021, **38**, p 101778
28. T.D. Ngo, A. Kashani, G. Imbalzano, K.T.Q. Nguyen, and D. Hui, Additive Manufacturing (3D Printing): A Review of Materials, Methods, Applications and Challenges, *Compos. B Eng.*, 2018, **143**, p 172–196
29. C. Burkhardt, P. Freigassner, O. Weber, P. Imgrund, S. Hampel, (2016) Fused filament fabrication (FFF) of 316L Green Parts for the MIM process, *World PM2016-AM-Deposition Technologies*,
30. X. Kan, D. Yang, Z. Zhao, and J. Sun, 316L FFF Binder Development and Debinding Optimization, *Mater. Res. Express*, 2021, **8**(11), p 116515